Computationally Efficient Model for Simulation of Boost Converter

B. Saritha, Vineet Pandey, G. Narayanan
Department of Electrical Engineering, Indian Institute of Science, Bangalore - 560012, INDIA
Email: saritha@ee.iisc.ernet.in, pandeyvineet45@gmail.com, gnar@ee.iisc.ernet.in

***Abstract*— This paper presents a computationally efficient model for a dc-dc boost converter, which is valid for continuous and discontinuous conduction modes; the model also incorporates significant non-idealities of the converter. Simulation of the dc-dc boost converter using an average model provides practically all the details, which are available from the simulation using the switching (instantaneous) model, except for the quantum of ripple in currents and voltages. A harmonic model of the converter can be used to evaluate the ripple quantities. This paper proposes a combined (average-cum-harmonic) model of the boost converter. The accuracy of the combined model is validated through extensive simulations and experiments. A quantitative comparison of the computation times of the average, combined and switching models are presented. The combined model is shown to be more computationally efficient than the switching model for simulation of transient and steady-state responses of the converter under various conditions.**

Keywords— Average model, boost converter, combined model, dc-dc converter, harmonic model, simulation of converters, switching model.

I. Introduction

DC-DC converters are often important subsystems in large systems such as electric vehicles [1, 2] and on-board ship power system [3]. Offline and real-time simulations of such large systems are carried out widely to study the feasibility, stability and performance of these systems [4, 5]. Such simulations require computationally efficient models for the various subsystems including power electronic converters.

The challenges in the computer based simulation of power electronic systems are described in [6]. For converters switching at high frequency, the simulation time step needs to be much shorter than the switching cycle. Hence the computation time required by the switching model is too high. Also, the resource consumption is enormous for such simulations.

Average model (wherein the various electrical quantities of the converter are averaged over each switching period) can be considered for simulation/performance evaluation of power converters in large systems [7]. State-space based average modeling of dc-dc converters are well explained in [8]-[10]. Tools for average modeling have been developed which can combine numerous modeling techniques such as large-signal, small-signal and equivalent circuit models [11].

Certain models impose restrictions such as operation of converter in the continuous conduction mode (CCM) only [11]. Quite often, practical applications require a converter to operate over a wide range of conditions, which could include continuous conduction mode and discontinuous conduction mode (DCM) [12]. Hence, a model should be applicable for both CCM as well as DCM. Moreover, the model should incorporate all non-idealities inclusive of equivalent series resistance (ESR) of capacitor, on-state drop of devices, series/internal resistance of inductors and power sources. The non-idealities have significant impact on the performance of the converter. Further, the model should be computationally efficient. This paper proposes a computationally efficient model of a boost converter which is applicable for CCM and DCM, and is capable of incorporating significant non-idealities.

Computational effort and resources required for simulation are significantly low in case of average model, compared to switching model [13]. This paper presents a quantitative comparison of the switching and average models of a boost converter in terms of accuracy and computation. The two models are compared, considering various scenarios such as different steady state operating conditions and different transients.

The average model is not capable of predicting the ripple in different currents and voltages, which could be significant under certain conditions, particularly in DCM. Hence, a harmonic model for the boost converter is also discussed in this paper. Further, a combined average-cum-harmonic model of boost converter is proposed in this paper. The switching, average and harmonic models are discussed in section II. Comparative results for the models, in terms of computation time and accuracy, are presented and summarized in section III. The accuracy of the models is verified through experiments on a 40 W boost converter prototype. The corresponding simulation and experimental results are presented in section IV.

II. Modeling of Boost Converter

A circuit schematic of the boost converter is shown in Fig. 1. The diode is represented as a series combination of forward drop V_f and an ideal diode D_{io}. MOSFET is

This work was supported by the Department of Heavy Industry, Government of India, under the project entitled “Development of offline and real time simulators for electric vehicle / hybrid electric vehicle systems”.

represented as a series combination of resistance R_{ds} and an ideal switch SW. The variables and parameters of the model are defined in Table I. The switching, average and harmonic models of the converter are discussed in this section.

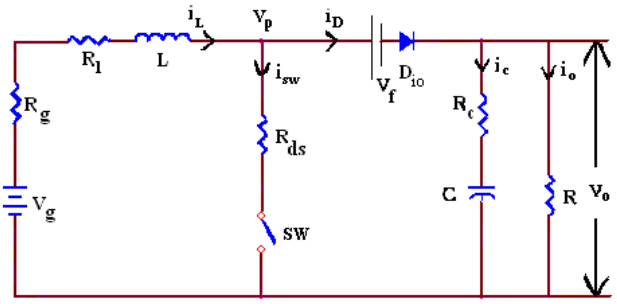

Fig. 1. Circuit schematic of a boost converter inclusive of significant non-idealities

TABLE I. PARAMETERS OF CONVERTER MODEL

Input variable	**Output variable**	**Model parameters**	**Parameter values**
Input voltage (Vg)	Output voltage (v_0)	Inductor (L)	2 mH
Duty cycle (D)	Output current (i_0)	Capacitor (C)	10 µF
	Inductor current (i_L)	Load (R)	105 Ω
	Output ripple voltage (ΔV_0)	Drop across diode (V_f)	0.8 V
	Inductor ripple current (ΔI_L)	ON resistance of switch (R_{ds})	55 m Ω
		Resistance of inductor (R_l)	2 Ω
		ESR of capacitor (R_c)	0.6 Ω
		Source Resistance (R_g)	1m Ω

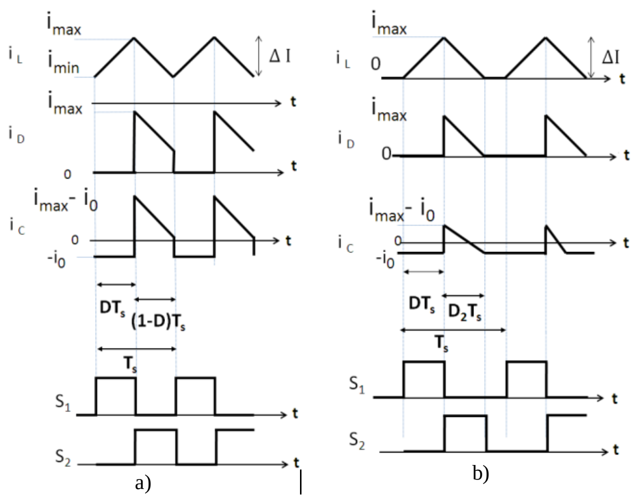

Fig. 2. Inductor current, diode current, capacitor current and switching functions of boost converter under a) CCM and b) DCM

A. Switching Model of Boost Converter

In the switching model of boost converter, the ON/OFF conditions of the MOSFET SW and diode D_{io} are represented by the switching functions S_1 and S_2, respectively. When the switching function is high (say S_1=1), the device (say MOSFET) is ON, and *vice versa*. As seen in Fig. 2, the conduction through the inductor L is continuous and discontinuous, during CCM and DCM, respectively. The switching functions S_1 and S_2 for CCM and DCM are illustrated in Fig. 2a and Fig. 2b, respectively. Under CCM, the switching function S_2 is the complement of S_1 i.e. $S_2 = \overline{S_1}$. Under DCM, the switching function $S_2 = 1$ if ($S_1 = 0$ and $i_D > 0$); else $S_2 = 0$.

Under CCM, the node voltage across the switch (v_p) and diode current (i_D) of an ideal boost converter can be expressed as:

$$v_p = v_0\ \overline{S_1} \tag{1}$$

$$i_D = i_L\ \overline{S_1} \tag{2}$$

Under DCM, the variables v_p and i_D are expressed in terms of S_1 and S_2, as given below:

$$v_p = v_0\ \overline{S_1}\ S_2 + V_g\ \overline{S_1}\ \overline{S_2} \tag{3}$$

$$i_D = i_L\ \overline{S_1}\ S_2 \tag{4}$$

It can be noted that the variable v_p is a function of both V_g and v_0. Equations (1) to (8) represent the switching model of the ideal boost converter under CCM and DCM operation.

$$\frac{di_L}{dt} = \frac{(V_g - v_p)}{L} \tag{5}$$

$$i_c = i_D - i_o \tag{6}$$

$$i_c = C\frac{dv_0}{dt} \tag{7}$$

$$i_0 = \frac{v_0}{R} \tag{8}$$

The non-idealities such as V_f, R_{ds}, R_c, R_l and R_g are considered in the simulation of non-ideal converter. The variables v_p and i_D of non-ideal boost converter operating under CCM are expressed as:

$$v_p = i_L R_{ds} S_1 + (v_0 + V_f)\ \overline{S_1} \tag{9}$$

$$i_D = i_L\ \overline{S_1} \tag{10}$$

Under DCM, the expression for v_p and i_D in (3) and (4), are generalized to incorporate all non-idealities as:

$$v_p = i_L R_{ds} S_1\overline{S_2} + (v_0 + V_f)\ \overline{S_1}\ S_2 + V_g\ \overline{S_1}\ \overline{S_2} \tag{11}$$

$$i_D = i_L\ \overline{S_1}\ S_2 \tag{12}$$

If the condition $S_1 = \overline{S_2}$ is imposed on DCM equations (11) and (12), the corresponding CCM equations (9) and (10) can be obtained.

The switching model of non-ideal boost converter is realized using the following equations, in addition to (9) and (10) or (11) and (12), depending on the operation in CCM or DCM:

$$\frac{di_L}{dt} = \frac{(V_g - v_p - i_L(R_l + R_g))}{L} \tag{13}$$

$$i_c = i_D - i_o \tag{14}$$

$$i_c = C\frac{dv_c}{dt} \tag{15}$$

$$v_c = v_0 - i_c R_c \tag{16}$$

$$i_0 = \frac{v_0}{\mathrm{R}} \tag{17}$$

TABLE II. EQUATIONS FOR AVERAGE MODEL OF BOOST CONVERTER

	Ideal boost converter	
	CCM	DCM
V_p	$V_0\,(1-D)$	$V_0 D_2 + V_g\,(1-D-D_2)$
I_D	$I_L\,(1-D)$	$I_L D_2$
	Boost converter with non-idealities	
	CCM	DCM
V_p	$I_L R_{ds} D + \{(V_0+V_f)*(1-D)\}$	$I_L R_{ds} D + \{(V_0+V_f)D_2\} + V_g\,(1-D-D_2)$
I_D	$I_L\,(1-D)$	$I_L D_2$

The switching model is simulated in MATLAB using the block diagram, shown in Fig. 3.

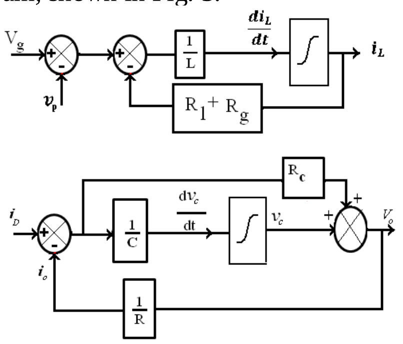

Fig. 3. Block diagram representation of non-ideal boost converter

B. Average Model of Boost Converter

While the switching (instantaneous) model relates the various instantaneous quantities in the converter, the average model relates the average voltages and currents; the voltages and currents are averaged over each switching cycle. The average voltages and currents are represented in capital letters, in order to differentiate them from the instantaneous quantities.

The duty cycle D (i.e. switching function S_1 averaged over a carrier period) is the control input to the model (Fig. 2). The expressions for V_p and I_D can be obtained by averaging the corresponding expressions of the switching model (1)-(4) and (9)-(12), over a switching period T_s. The expressions for V_p and I_D are tabulated in Table II. Under ideal conditions, the duty ratio D_2 of diode, used in Fig. 2 and Table II, can be expressed as [8]:

$$\mathrm{D}_2 = \frac{\mathrm{K} + \sqrt{\mathrm{K}^2 + 4\mathrm{D}^2\mathrm{K}}}{2\mathrm{D}};\ \text{where } \mathrm{K} = \frac{2\mathrm{L}}{\mathrm{RT_s}} \tag{18}$$

Even in the presence of non-idealities, the above expression is found to be reasonably valid. D_2 is the value obtained by averaging the switching function S_2 over a carrier period T_s. V_p and I_D are fed into the block diagram in Fig. 3 (instead of v_p and i_D), to solve the average model of boost converter.

C. Harmonic Model of Boost Converter

The harmonic model relates the ripple quantities (switching frequency components) in different currents and voltages of the converter. As illustrated in Fig. 2, the inductor current (i_L), multiplied by the switching function S_2, gives the diode current (i_D). The average of i_D (i.e. dc component of diode current) flows through the load (i_0) and the ripple component flows through the capacitor (i_c). The relationship among i_D, i_0 and i_c are shown by Fig. 2.

In general, the peak-peak ripple in inductor current (ΔI_L) can be expressed as:

$$\Delta \mathrm{I_L} = \mathrm{I_{max}} - \mathrm{I_{min}} = \left|\frac{\mathrm{di_L}}{\mathrm{dt}}\right|_{\mathrm{ON}} * \mathrm{DT_s} \tag{19}$$

where I_{max} and I_{min} are maximum and minimum values, respectively, of the inductor current, as depicted in Fig. 2a. For DCM, $I_{min} = 0$. Further $\left|\frac{di_L}{dt}\right|_{ON}$ is the average value of $\frac{di_L}{dt}$ over the ON duration of the switch SW (i.e $0 < t < DT_s$) and can be expressed as:

$$\left|\frac{\mathrm{di_L}}{\mathrm{dt}}\right|_{\mathrm{ON}} = \frac{\mathrm{V_g} - \mathrm{I_{L1}R_{non}}}{\mathrm{L}};\quad \mathrm{R_{non}} = \mathrm{R_g} + \mathrm{R_l} + \mathrm{R_{ds}} \tag{20}$$

where I_{L1} is the average inductor current during the ON-state of switch SW. Based on Fig. 2, for CCM and DCM conditions, I_{L1} can be expressed as shown in (21) and (22), respectively.

$$\mathrm{I_{L1}} = \frac{\mathrm{I_{max}} + \mathrm{I_{min}}}{2} = \mathrm{I_L};\ \text{CCM} \tag{21}$$

$$\mathrm{I_{L1}} = \frac{\mathrm{I_{max}}}{2} = \frac{\mathrm{I_L}}{\mathrm{D+D_2}};\quad \text{DCM} \tag{22}$$

For an ideal converter, $\left|\frac{di_L}{dt}\right|_{ON}$ reduces to $\frac{V_g}{L}$. The value of ripple in inductor current (ΔI_L) is evaluated using (19)-(22), where I_L, D and D_2 can be obtained from the average model. The ripple voltage across the capacitor is caused by the capacitor current i_c. The capacitor current and ripple voltage for CCM and DCM are illustrated in Fig. 4 and Fig. 5, respectively. In Fig. 4a, the converter is operating under CCM, and I_{min} is greater than load current I_o. The capacitor current during the ON duration is I_o. Hence the peak-peak ripple voltage (ΔV_c) across the capacitor is written as:

$$\Delta V_c = \frac{\mathrm{I_o} D T_s}{C} = \frac{\mathrm{V_o}}{\mathrm{R}}\frac{D T_s}{C} \tag{23}$$

When the converter is operating under CCM, and the minimum inductor current I_{min} is less than load current I_o, the current through the capacitor is as shown in Fig. 4b. Considering the flow of capacitor current in one direction, ΔV_c can be expressed as:

$$\Delta \mathrm{V_c} = \frac{(1-\mathrm{D})\ \mathrm{T_s}}{2\ \mathrm{C}} \frac{(\mathrm{I_{max}} - I_0)^2}{\mathrm{I_{max}} - \mathrm{I_{min}}} \tag{24}$$

where $I_{max} = I_L + \Delta I_L/2$ and $I_{min} = I_L - \Delta I_L/2$.

When the converter is operating under CCM, and the minimum inductor current I_{min} is less than load current I_o, the current through the capacitor is as illustrated by Fig. 4b. Considering the flow of capacitor current in one direction, ΔV_c can be expressed as:

$$\Delta V_c = \frac{(1-D)\,T_s}{2\,C}\,\frac{(I_{max}-I_0)^2}{I_{max}-I_{min}} \tag{24}$$

where $I_{max} = I_L + \Delta I_L/2$ and $I_{min} = I_L - \Delta I_L/2$.

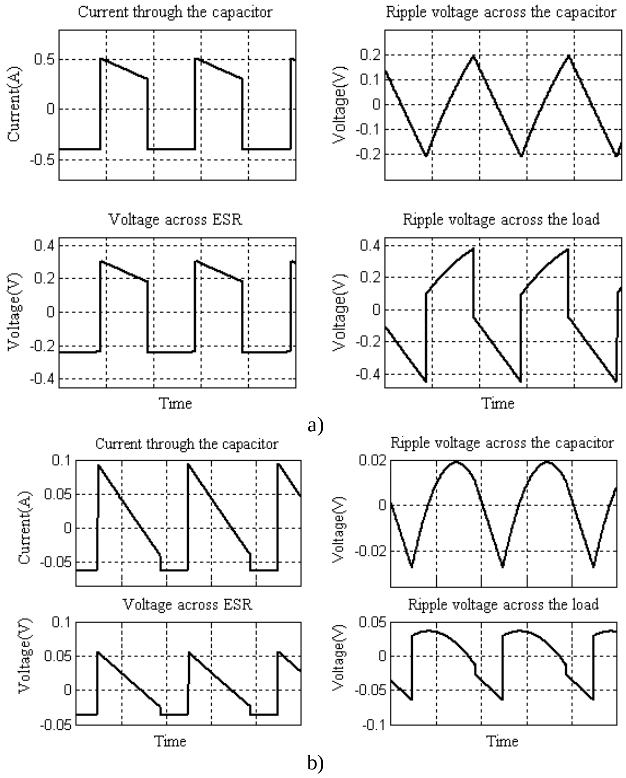

Fig. 4. Ripple voltages in a boost converter operating under CCM when a) $I_{min} > I_0$ and b) $I_{min} < I_0$

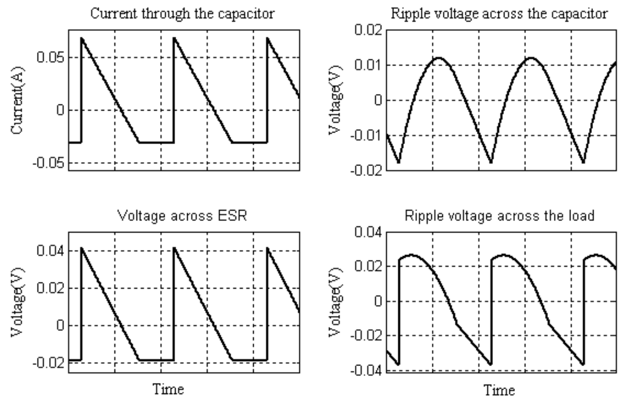

Fig. 5. Ripple voltages in a boost converter operating under DCM

When the converter is operating under DCM, the capacitor current is as shown in Fig. 5. The ripple voltage ΔV_c is given by:

$$\Delta V_c = \frac{D_2\,T_s}{2\,C}\,\frac{(I_{max}-I_0)^2}{I_{max}} \tag{25}$$

Where $I_{max} = \Delta I_L$. This can be derived from (24) by substituting (1-D) by D_2 and $I_{min} = 0$. For an ideal converter, the peak-peak output voltage ripple (ΔV_0) is equal to ΔV_c. When the ESR of capacitor (Rc) is significant, the peak voltage drop across R_c is given by $I_{max}*R_c$. The peak voltage drop across R_c is added to ΔV_c, to obtain the output voltage ripple ΔV_0, as shown below:

$$\Delta V_o = \Delta V_c + I_{max} * R_c \tag{26}$$

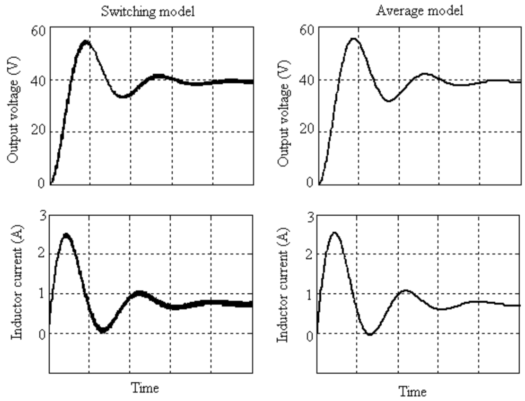

Fig. 6. Simulation results showing the startup transients in boost converter

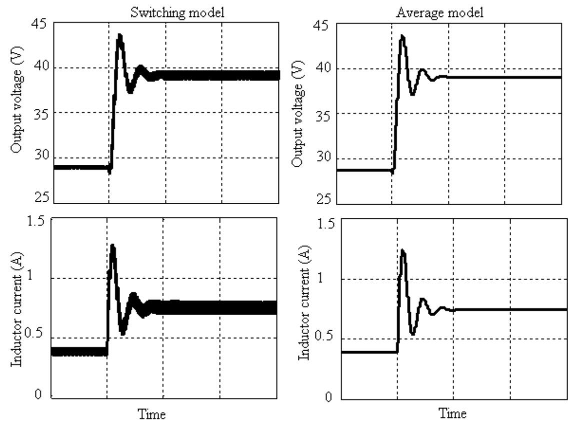

Fig. 7. Simulation results for change in D from 0.3 to 0.5; R = 105Ω; V_g = 21.4 V

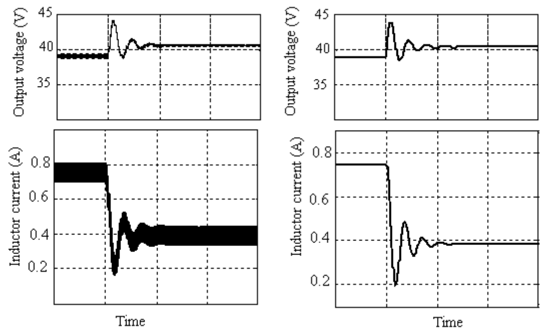

Fig. 8. Simulation results for change in R from 105 to 210 Ω; D=0.5; V_g = 21.4 V

D. Comparison of dynamic performance of models

The boost converter is simulated in MATLAB using the parameters, listed in Table I. The converter is operated at 50 kHz switching frequency and 50% duty cycle. The input voltage of the converter V_g is 21.4 V, and load resistance R is 105 Ω. The startup transients of the converter, obtained from average and switching models, are shown in Fig. 6. When duty cycle is varied from 0.3 to 0.5, the corresponding output voltage and inductor current are shown in Fig. 7. The transient response for a change in load resistance from R=105Ω to R=210Ω, is shown in Fig. 8.

Fig. 6 to Fig. 8 show clearly that the average model is comparable to the switching model in predicting the dynamics of the boost converter. The magnitude of ripple in currents and voltages are obtained from harmonic model of the converter. Hence, the combined average-cum-harmonic model can be considered as a good alternative to the switching model.

III. Comparative Evaluation of Computation Time

The boost converter is driven at 50 kHz. The switching model is run with a time step of 1e-7 sec (i.e. 0.005*T_s), which is much lower than the switching period T_s. Since the average model concerns only switching-cycle-averaged quantities, the time step could be significantly higher than that of the switching model. The time step of 1e-5 sec (i.e. 0.5*T_s) is chosen here for both the average model and the combined (average + harmonic) model.

TABLE III. Comparison of Computation Time for Startup Condition of Boost Converter

Operating condition				**Computation time (sec)**		
Duty cycle D	Load R Ω	Mode CCM/ DCM	Time period (msec)	Switching Model	Average Model	Average+ Harmonic Model
0.5	105	CCM	10	5.269	0.262	0.314
0.2	1600	DCM	40	20.85	0.469	0.769

TABLE IV. Comparison of Computation Time for Steady-state Operating Condition of Boost Converter

Operating condition			**Computation time (sec)**		
Duty cycle D	Load R Ω	Mode CCM/DCM	Switching Model	Average Model	Average+ Harmonic Model
0.5	105	CCM	45.93	0.747	1.057
0.8	105	CCM	45.32	0.706	0.879
0.5	1600	DCM	46.13	0.643	0.705
0.2	1600	DCM	40.27	0.524	0.655

TABLE V. Comparison of Computation Time for Transient Condition of Boost Converter

Transition	**Conduction mode CCM/DCM**	**Computation time (sec)**		
		Switching Model	Average Model	Average + Harmonic Model
Step change in D from 0.3 to 0.5; R = 105 Ω	CCM	4.537	0.0707	0.177
Step change in D from 0.7 to 0.2; R=105 Ω	CCM	4.863	0.0814	0.101
Step change in R from 105 Ω to 210 Ω; D=0.5	CCM	4.855	0.077	0.106
Step change in R from 800 Ω to 200 Ω ; D=0.5	CCM	4.818	0.07	0.088
Step change in R from 105 Ω to 1750 Ω; D=0.5	CCM to DCM transition	5.872	0.078	0.0875
Step change in D from 0.3 to 0.5; R = 1750 Ω	DCM	4.761	0.0795	0.2351
Step change in D from 0.7 to 0.2; R=1750 Ω	DCM	4.97	0.0815	0.2433
Step change in R from 1750 Ω to 2000 Ω ; D=0.5	DCM	5.141	0.0396	0.2071
Step change in R from 2200 Ω to 1800 Ω ; D=0.5	DCM	4.778	0.0355	0.1321
Step change in R from 1750 Ω to 105 Ω; D=0.5	DCM to CCM transition	4.7313	0.0368	0.2216
Step change in V_g from 21.4 to 25 V; R=105 Ω; D=0.5	CCM	4.7157	0.0672	0.2627
Step change in V_g from 21.4 to 25 V; R=1750 Ω; D=0.2	DCM	4.9078	0.0436	0.1843
Step change in V_g from 25 to 21.4 V; R=105 Ω; D=0.5	CCM	5.339	0.0628	0.0781
Step change in V_g from 25 to 21.4 V; R=1750 Ω; D=0.2	DCM	4.604	0.0484	0.2277

The computation times for simulating the start-up transients, starting from zero initial conditions, for D=0.5 (CCM operation) and D=0.3 (DCM operation) are tabulated in Table III. The simulations are carried out up to 10 ms and 40 ms, respectively for the two cases. As seen, the average model and the combined model consume much less computation time than the switching model. Similar observations can be made regarding the simulation of steady-state responses for duration of 90 ms (Table IV) and for simulation of various transient responses (Table V). The transients considered include step changes in D, step changes in R, and step changes in V_g for CCM as well as DCM conditions. The measured computation times in Table III to V are consistent in showing a very significant reduction in computation time with the average and combined models, compared to the switching model.

TABLE VI. Comparison Between Experimental and Simulation Results

1. Continuous conduction mode (CCM)			
Parameters	**D=0.52**		
	Experimental Results	Average + Harmonic model	Switching Model
V_o	40.8 V	40.54 V	40.8 V
I_o	0.38 A	0.38 A	0.38 A
I_L	0.8 A	0.8 A	0.8 A
ΔI_L	0.12 A	0.1027 A	0.1 A
ΔV_c	1 V	0.911 V	0.854 V
R	105 Ω	105 Ω	105 Ω
2. Boundary condition between CCM and DCM			
Parameters	**D=0.52**		
	Experimental Results	Average + Harmonic model	Switching Model
V_o	43.6 V	43.54 V	43.99 V
I_o	0.024 A	0.0272 A	0.0274 A
I_L	0.057 A	0.055 A	0.0567 A
ΔI_L	0.11 A	0.1105 A	0.1135 A
ΔV_c	0.1 V	0.0955 V	0.078 V
R	1600 Ω	1600 Ω	1600 Ω

3.Discontinuous conduction mode (DCM)			
Parameters	**D=0.22**		
	Experimental Results	Average + Harmonic model	Switching Model
V_o	27.5V	26.922V	27.25V
I_o	0.017A	0.0168A	0.01707A
I_L	0.022A	0.0228A	0.022A
ΔI_L	0.05A	0.047A	0.048A
ΔV_c	0.04V	0.038V	0.03V
R	1600 Ω	1600Ω	1600Ω

IV. Experimental Verification of Accuracy

A 40 W boost converter prototype is built to verify the accuracy of the simulation models. The steady state results from the switching model and experiment are compared in Fig. 9. The converter is operated under various conditions, as indicated by Table VI; the measurements are tabulated along with the simulation results. As seen, the simulation results closely match with the experimental data.

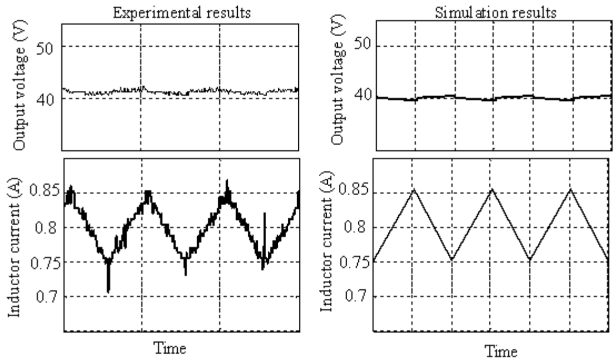

(a)

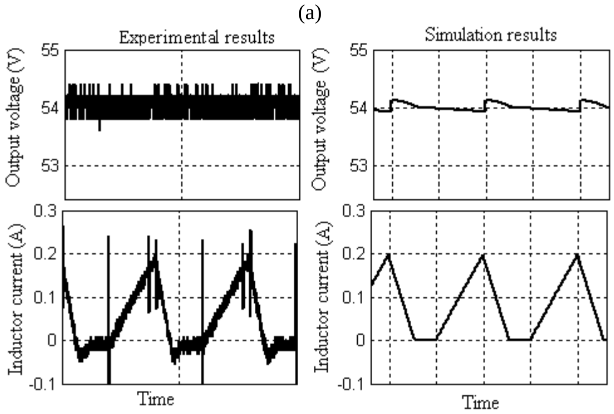

(b)

Fig. 9. Verification of simulation results with experiment: steady-state operating condition of converter; a) V_g = 21.6 V, D = 0.51, R = 102.6Ω, f_{sw} = 50 kHz; b) V_g = 20 V, D = 0.5, R = 1980Ω, f_{sw} = 25 kHz

V. Conclusion

The switching (instantaneous), average and harmonic models of a dc-dc converter are discussed. The models are suitable for both CCM and DCM, and also can incorporate non-idealities in the converter. A combined average-cum-harmonic model is proposed in this paper. For a detailed comparative study, the switching, average and combined models are used to simulate the transient and steady-state behavior of the boost converter under various conditions. The computation times consumed by the three models are measured and compared.

The accuracies of the various models are validated using experimental results. Simulation results based on combined model tally with those based on switching model. While the combined model provides almost all details of practical interest as are available from the switching model, this model consumes much lower time than the switching model for simulation of various steady-state and transient responses. The computation time consumed by the combined model is only slightly higher than that of the average model. The combined (average-cum-harmonic) model is recommended for simulation of dc-dc converters, as part of large systems such as electric vehicles. The work in this paper is also of tutorial significance to students and engineers.

References

[1] I.A. Khan, "DC-to-DC converters for electric and hybrid vehicles ", *IEEE Proc. Power electronics in transportation*, 1994, pp. 113-122.

[2] D.M. Bellur and M.K. Kazimierczuk, "DC-DC converters for electric vehicle applications", *Proc. Electrical insulation conference and electrical manufacturing expo*, 2007, pp. 286-293.

[3] Il-Yop Chung, Wenxin Liu, Mike Andrus, Karl Schoder, Siyu Leng, David A. Cartes, and Mischa Steurer, "Integration of a bi-directional dc-dc converter model into a large-scale system simulation of a shipboard MVDC power system", *Proc. IEEE Electrci Ship Technology Symposium*, 2009, pp. 318-325.

[4] W. Ren, M. Steurer and S. Woodruff, "Applying controller and power hardware-in-the-loop simulation in designing and prototyping apparatuses for future all electric ship", *Proc. IEEE Electric Ship Technologies Symposium*, 2007, pp. 443-448.

[5] Soo-Nam Kim, P. Stone, Y. Zhang, Yong-June Shin and R. Dougal, "Evaluation of power system design for an electric ship with VTB dynamic generation model", *Proc. IEEE Electric Ship Technologies Symposium 2011*, pp. 150-155.

[6] V. J. Thottuvelil, "Challenges in computer-based analysis/ simulation and design of power electronic circuits," *Proc. 1988 IEEE Workshop on Computers in Power Electronics*, pp. 1-8.

[7] M.M. Jalla, A. Emadi, G.A. Williamson and B. Fahimi, "Real time state estimation of multi-converter more electric ship power systems using the generalized state space averaging method", *IEEE IECON 2004*, pp. 1514-1519.

[8] Erickson, W. Robert and Dragan Maskimovic, "AC Equivalent Circuit Modeling" in "*Fundamentals of power electronics*",2nd ed,Springer, 2001, ch. 7, sec. 7.3, pp. 213-226

[9] M.B.Patil, V.T.Ranganathan and V. Ramanarayanan, "Dynamic Performance of Switched Mode Power Converters" in "*Simulation of power electronic circuits*", Narosa, New Delhi, 2009. ch.17, sec.17.9, pp.17.9-17.19

[10] N. Mohan, T.M. Undeland and W.P. Robbins, "Switching DC Power Supplies" in "*Power electronics: converters, applications, and design*", Wiley Student Edition, 3rd ed, New Delhi, India, 2007. ch. 10, sec. 10-5, pp. 322-341.

[11] Asma Merdassi, Laurent Gerbaud and Seddik Bacha,"A new automatic average modeling tool for power electronic systems", IEEE PESC'2008, pp. 3425-3431.

[12] T. Hwang and S. park, "Seamless boost converter control under the critical boundary condition for a fuel cell power conditioning system", *IEEE Trans. Power Electronics*, vol. 27, no. 8, Aug. 2012, pp. 3616-3626.

[13] K. Gorecki, J. Zarebski and R. Zarebski, "Investigations of Usefulness of Average Models for Calculations Characteristics of the Boost Converter at the Steady State", *Proc. Int. Conf. Modern problems of radio engineering, telecommunications and computer science*, 2008, pp.163-166.